System Integration Based on Micro-Nanotechnology and Biomedical Applications

Fumihito Arai

Professor
Department of Bioengineering and Robotics, Graduate School of Engineering
E-mail: arai@imech.mech.tohoku.ac.jp

1. Introduction of Mechano-Bio Systems

Mechano-bio systems play an important role to supply advanced devices and equipments for biomedical engineering. The need of the mechano-bio systems is increasing for technological innovation and micro-nano technology is indispensable for miniaturization as well as functionalization. In this project, we study on mechano-bio systems integrated by using micro-nanotechnology.

Mechano-bio systems are defied as (1) the systems which deal with the molecules, cells, and tissues mechanically, (2) the artificial systems which mimic the biological elements or life itself, and (3) the hybrid systems or devices which introduce the biological elements or life into the artificial devices or the biocompatible systems which are taken into the biological object.

Common technical interest will be the micro and nanotechnology in designing and producing the system and bio-compatibility of the system. Micro-nanotechnology plays an important role for system integration. Here we introduce our recent works. Here we introduce part of our research activites.

2. Manipulation of Micro-nano Scale Biological Objects

2.1. Noncontact manipulation in a chip by optical tweezers

On-chip single cell analysis is an important approach for research and development in life science, pharmaceutical industry, livestock agriculture, and so on. Optical tweezers are well known as one of the noncontact manipulation methods used in a closed space and much has been reported. Optical tweezers are suitable to manipulate a single micro to nano scaled particle. Direct laser manipulation is not recommended for cell manipulation and advantage of using microtools was shown by the author [1]. We achieved three-dimensional 6 DOF manipulation of the laser trapped object [2]. Recent research attention has been gathered dexterous manipulation. This year, we proposed novel manipulation method integrating multiple laser beams. We succeeded in manipulation of microtools made by photolithography (Fig. 1) and functional gel microtools [3].

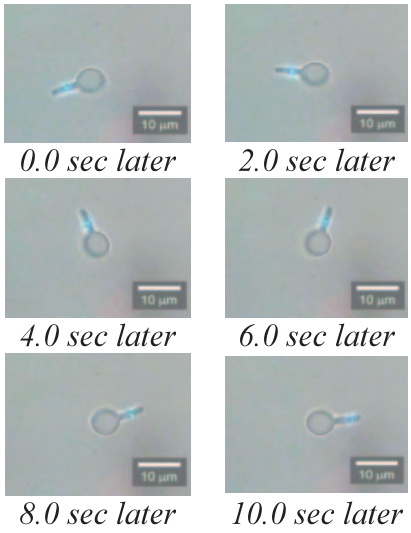

Fig. 1. Manipulation of a microtool with IOT

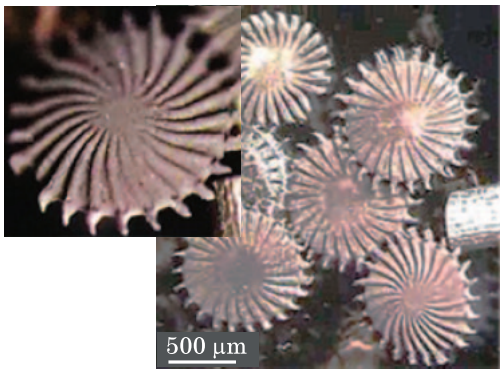

Fig. 2. Example of 3D MMT

2.2. Noncontact manipulation in a chip by Magnetically Driven Microtools

It is desired to have actuators which have the ability of enough actuation force to manipulate cells as well as the softness enough to be harmless to actuate cells. We proposed a magnetically driven microdevice for making a disposable microchip with simple control. We reported novel polymeric magnetically driven microtools (MMT) for non-intrusive and no contamination experiments on a chip [4]. The composites were formed by suspending magnetite nanoparticles in polydimethylsiloxane (PDMS). This year, we improved the system by using 3D fabrication of MMT (Fig. 3) [5] and magnetic field concentration

for powerful actuation. We applied it for several on-chip applications [6].

3. Exoskeletal Microarm for Endoscopy

As cancer becomes the No.1 cause of the death in Japan, endoscopic surgery is gaining attentions. We proposed an endoscopical tool to manipulate and peel tumor skin in ESD (Endoscopic Submucosal Dissection). This microarm will come out from the tip of an endoscope to help the manipulation of the tumor skin. The concept diagram of the microarm is shown in Fig. 3. The microarm is composed of 5 layer parts and the central plate is used as spring to bend. This research needs to emphasize a new fabrication method of arm which is fabricated by photolithography and electroplating.

Assembly of small parts is always difficult. Here, we proposed a new method of assembly called STAMP (Stacking Microassembly Process) which enables to produce 3-Dimensional structure by stacking 2-Dimensional layer parts (Fig. 4) [7]. The microarm uses the elastic deformation of metal to bend. The fifth sensor layer is articular joint being fabricated by using plate spring. We used a commercially available strain gauge (KFG-1-120-C1-16L3M3R, KYOWA) which is placed on the joint as an angle sensor. The sensor can be fabricated by patterning polyimide and Pt/Au, and wired by patterning Au.

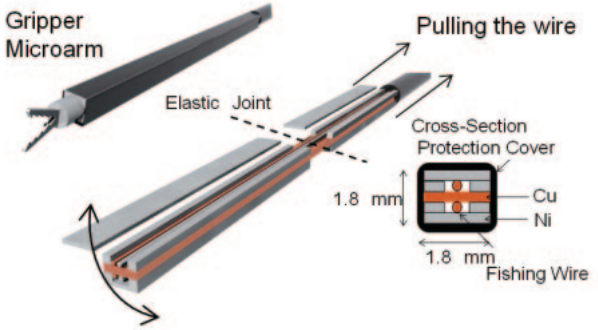

Fig. 3. Structural diagram of the microarm

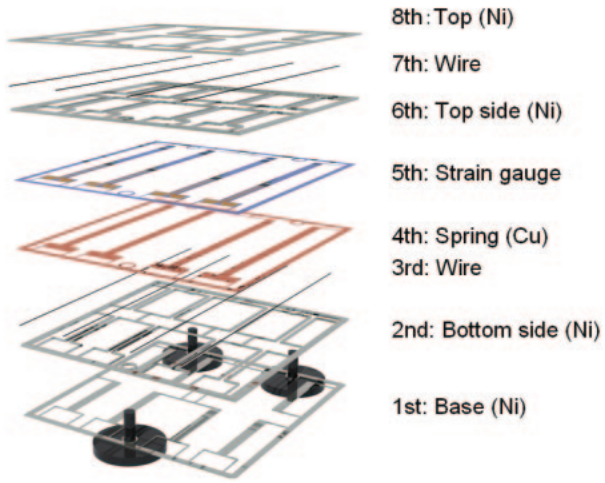

Fig. 4. Stacking Microassembly Process (STAMP)

Here, we describe the fabrication method of each layer. Instead of using machining or wire cutting, we used photolithography and electroplating because it can be shaped into any form with high resolution (20 μm, patterning the SU-8 to 100 μm in height with the aspect ratio of 5) with mass productivity [7]. We decided to use Ni electroplating for the structure of the microarm. Ni is bio-compatible, meaning it is not harmful to put inside a human body. As for the spring of the microarm, Cu electroplating is employed at first.

The fabrication process is shown in Fig. 5. First, sacrificial layer of LOR 5B (Micro Chem) is spin coated onto 35x35 mm clean Si wafers. We, then, sputter deposit Cr/Au onto the sample, aiming to the thickness of 50 nm and 150 nm, respectively. Then, we spin coat the thick negative photoresist (SU-8, MicroChem), and exposed the I-line (365 nm) on top of the emulsion mask using SUSS (MicroTec AB, MA6). The patterned sample was placed in a nickel sulfamate acid bath for the electroplating. Area where there is no photoresist is electroplated and metal deposition is formed. Then, it was placed in RemoverPG (MicroChem) for 6 h to dissolve the LOR 5B, and lift off the fabricated structure. They are washed in ethanol and put in the ultrasonic bath to remove the debris of Cr/Au.

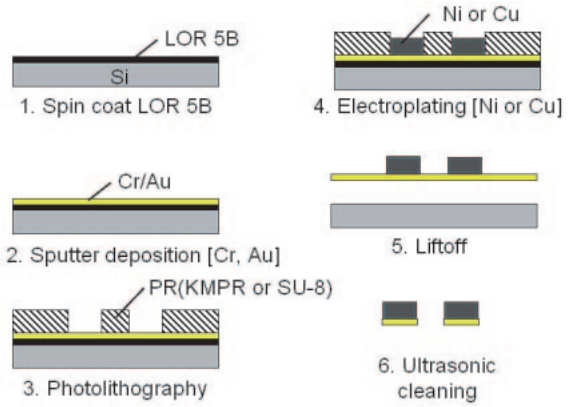

Fig. 5. Fabrication process

For the plate spring, we used a phosphor-bronze plate. It was impossible to electroplate phosphor-bronze, therefore, we used a dicing saw. The phosphor-bronze plate of thickness 0.1 mm was cut in the width of 1 mm. For more complicated structure, we can employ electric discharge machining and laser processing. Figure 6 shows the microarm.

The microarm bends using the elastic deformation of the phosphor bronze strip. We attached a commercial strain gauge as an angle sensor to measure the bending of the microarm. We are now working on fabricating the strain gauge layer to be able to assembly to the microarm using the STAMP. The output voltage of the strain gauge and the bending angle are in high linearity. It is feedback controlled with PID using a strain gauge attached to the articulated joint.

The gripper is fabricated and assembled by STAMP. Both gripper and microarm are confirmed of its movement.

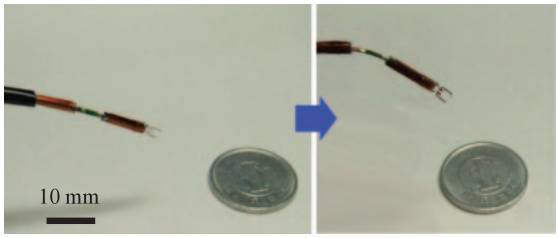

Fig. 6. Bilateral actuation of the microarm

4. Tailored Human Models and Scaffolds

We have developed scaffolds of three-dimensional (3D) synthetic vascular prostheses in tailor-made. Artificial carotid artery was made by combining processes of rapid prototyping, lost wax, dip coating, selective dissolution and salt leaching [8]. This scaffold is porous and made of biodegradable polymer. Human umbilical vein endothelial cells (HUVECs) are adhered to the inner surface of the scaffold for their anticoagulant effects.

We also developed arteriole and capillary vessel models [9,10]. Here we explain details of our works.

4.1. Fabrication of capillary vessel models with circular cross-section

In the tissue engineering field, many engineered approaches have been studied, including artificial hearts, artificial joints and synthetic vascular prostheses. We have been developing the three-dimensional(3D) elastic membranous blood vessel models in tailor-made by using 3D WAX models. We have been developing a surgical simulator by connecting the elastic membranous models. Surgical simulators are used in practice and rehearsal for catheter treatments and new treatment methods by doctors. Meanwhile, we constructed a pulsatile pump which can reproduce patient-specific pulsative blood streaming obtained by ultrasonic measurement or other modalities, connected it to the aorta model and reproduced human-like pulsatile blood streaming inside the simulator (vascular model can reproduce vascular pulsation with the streaming.).

We think arteriole and capillary vessel model is needed for more similar environment in surgical simulator. In this study, I fabricate arteriole and capillary vessel model for the purpose of building up surgical simulator.

There are diseases in under ϕ500 μm blood vessels, such as arteria basilaris, but previous surgical simulator is not suitable for rehearsal and training of these diseases. Therefore, surgical simulator with ϕ10 - 500 μm arteriole and capillary vessel models are needed. We have been designed arteriole and capillary vessel models. Arteriole and capillary vessel model channel is needed to create in 500 μm - 10 μm size.

In addition, synthetic vascular prosthesis smaller than 6 mm are difficult to develop, and we know little about cell behavior and morphology in arterioles and capillary vessels. Our fabricated an arteriole and capillary vessel models by photolithography to better understand cell behavior and morphology of cells in arterioles and capillary vessels.

After exposure, fabricated photoresist patterns are transcribed onto poly(dimethylsiloxane) (PDMS). Arteriole and capillary vessel models with circular cross section are completed by bonding two patterned PDMS substrates using plasma treatment and heating process (Fig. 4.1). We succeeded in making capillary vessel tube model. Branched capillary vessel tube model was about 10 μm diameter. Cross-section of capillary vessel model was nearly circular. But, this model's cross-section of channel has very little out of alignment (Fig. 4.2). To solve this problem, we fabricate capillary vessel model patterns and alignment patterns for assembly by multi stage exposure photolithography.

And as an application example of the capillary vessel model, we observed HUVECs behavior and morphology in 10 μm diameter microchannels.

A. Fabrication method

One of our goals is to make a carotid artery of dozens of mm blood vessels in caliber. We tried to fabricate arteriole and capillary vessel model with circular cross- section whose caliber is 1 mm - 10 μm (Fig. 4.3). Reflow method, grayscale lithography and over exposure method in photolithography process can make semiround pattern. Reflow method is simple method for making semiround patterns, but needed to find best heating time condition. Grayscale lithography is useful method for 3D structure patterns, but difficult to make grayscale masks. Over exposure method is simple method for making semiround patterns, but needed to find best exposure condition. And, we choose over exposure method in these methods.

Firstly, for making semiround resist patterns 10 μm in diameter, we experimented in pattern's circularity. This experiment process flow is the following.

- Coat a substrate with 8-μm-thick photoresist PMER P-LA900PM (800 ~1200 Doses).

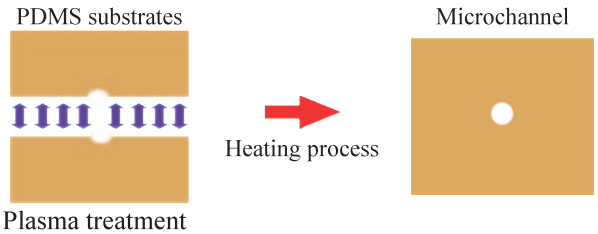

Fig. 4.1. Concept of making capillary vessel model. After plasma treatment, we align and bond two patterned PDMS substrates by heating and complete capillary vessel model.

- Over expose at soft-contact using both a mask and a resist sample until 1200, 1300, 1500, 1600, 1700, 1800, 1900 Doses.
- Develop for 5 minutes.
- Transcribe silicon pattern on PDMS.
- Observe the cross-section of transcribed PDMS.

Figure 4.4 shows circularity result at each exposed dose. In 1200~1400 Doses, the resist pattern shape is the trapezoid or triangular, and the circularity is low with about 60%. In 1500~1700 Doses, the resist pattern shape is the semiround, and the circularity is high with about 80%. In over 1700 Doses, the resist pattern shape is the oval, and the circularity falls fast until about 40%. (a) shows the peak at triangular shape, lowers afterwards the height part, and receives (b) that is the peak value at round shape in figure though are in the circularity two peak values of (a) and (b). The reason why the graph has increased and decreased is that the number of sampling to each light exposure was one time.

Figure 4.5 shows the patterned model for a channel and patterns for alignment. After transcribe the pattern on PDMS, we bond two PDMS substrates and complete capillary vessel model.
Process flow is the following.

- Coat a substrate with 8-μm-thick photoresist PMER P-LA900PM (800 ~1200 Doses).
- Expose at hard-contact using both a mask and a resist sample until 1000 Doses.
- Develop for 7 minutes.
- 145°C, 30min. hardbake.
- After using plasma hydrophilic treatment, coat a substrate with 8-μm-thick photoresist PMER P-LA900PM.
- Expose at hard-contact using both a mask and a resist sample until 1000 Doses.
- Develop for 7 minutes.
- 145°C, 30min. hardbake.
- After using plasma hydrophilic treatment, coat a substrate with 8-μm-thick photoresist PMER P-LA900PM.
- Expose at soft-contact using both a mask and a resist sample until 1500 Doses.
- Develop for 5 minutes.
- Transcribe silicon pattern on PDMS.

We observed Y branched channel pattern 4.5 x 10 μm (high x wide) in second step. And, there are the assembly alignment patterns, and each pattern is 7 μm, 8.5μm high, and 1 mm in diameter.

For simplicity, we transcribed resist patterns on PDMS to get concave patterns. We washed the patterned PDMS substrate with ethanol for 7 minutes twice to completely remove resist. Next, we transcribed the concave pattern on PDMS to get a convex patterned PDMS substrate for use as a master pattern. We transcribed the convex pattern on PDMS again to get a concave PDMS substrate for observing cell behavior and morphology. The PDMS substrate is easily reproduced using plasma hydrophilic treatment before printing. After plasma hydrophilic treatment, we aligned two patterned PDMS substrates under the microscope. After clamping the substrates, we bonded them at 145°C for 20 minutes, and completed the capillary channel. We experimented in flowing methyleneblue solution in the channel to check for leakage. The capillary channel had no leaks. And, we observed capillary channel had circular cross-section.

B. Evaluation of cross-section of fabricated model

We evaluated the model's cross-section alignment and channel's circularity about having alignment patterns for assembly and not having. We evaluated about (1) cross-section alignment and (2) channel's circularity. (1) is evaluated by drawing perpendicularly from the center of the semicircle to the bonded surface. In valuation of these model's out of alignment, a model having no alignment patterns is 2.5 μm out of alignment. And, a model having alignment patterns is 0.6 μm out of alignment. Alignment patterns improved cross-section alignment from 2.5 μm to 0.6 μm. (2) is evaluated by using the expression as circularity defined by the shortest axis divided by the longest axis. Using this expression, we calculated circularity of a model having no alignment patterns is 70%. And, we calculated circularity of a model having alignment patterns is 84%. Alignment patterns improved circularity from 70% to 84%.

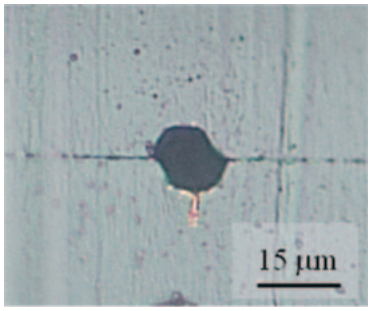

Fig. 4.2. Cross-section of capillary vessel model channel (before improvement).

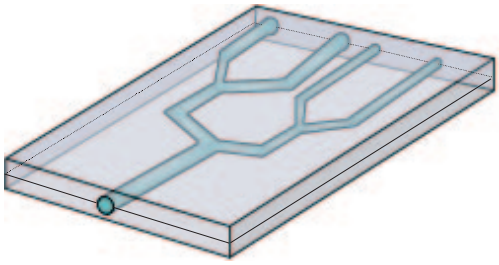

Fig. 4.3. Designed arteriole and capillary vessel model.

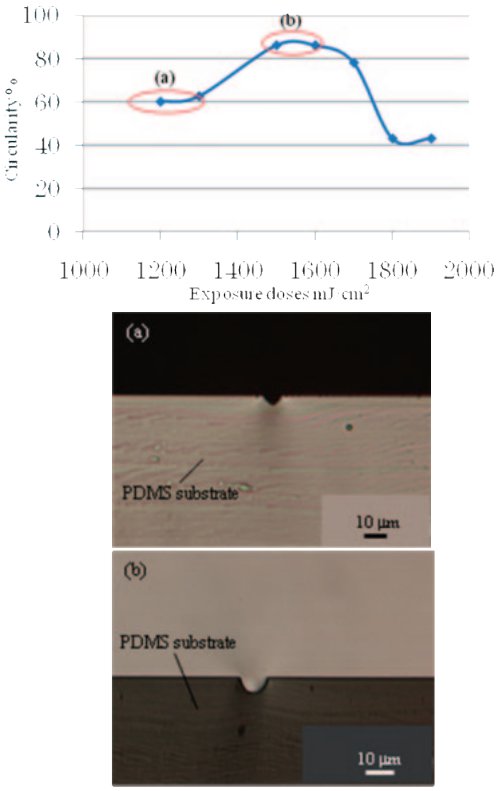

Fig. 4.4. Circularity result at each exposed dose. (a) shows the resist pattern shape is the trapezoid or triangular in 1200~ 1400 Doses. (b) shows the resist pattern shape is the semiround in 1500~ 1700 Doses.

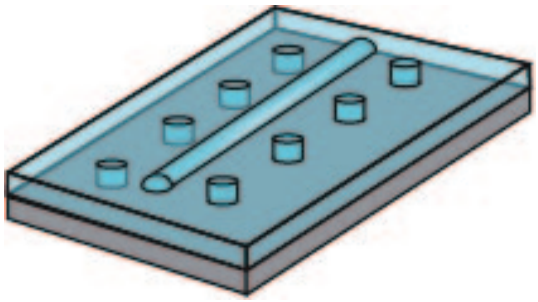

Fig. 4.5. Designed convex pattern for channel and patterns for alignment.

By evaluation results, alignment patterns for assembly improved cross-section alignment from 2.5 μm to 0.6 μm. And, alignment patterns improved channel's circularity from 70 % to 84%.

C. Application of capillary vessel models

We referred to previous observing reports about cells on microchannels, and incubated HUVECs on 10 μm diameter microchannels made by over exposure method and PDMS bonding. Purpose of this experiment was getting much knowledge about cell behavior and morphology on microchannels. The model for this experiment had no alignment

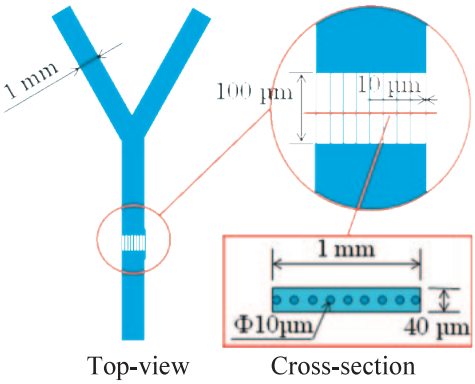

Fig. 4.6. Designed model for seeding and observing HUVEC experiment.

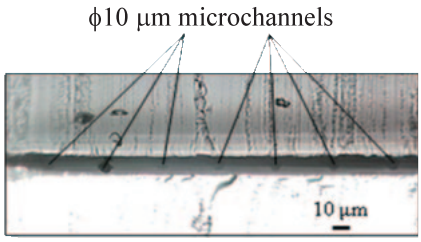

Fig. 4.7. Fabricated model's cross-section.

patterns for assembly. Figure 4.6 shows design concept. Designed channel has 1 mm wide Y branched shape and 10 μm diameter microchannels. We made this microchannels by multi stage exposure lithography. Process flow is the following.

(1) Fabrication step of 10 μm diameter microchannels

- After HMDS coating, coating 10-μm-thick PMER on silicon substrate.
- Expose at soft-contact using both a mask and a resist sample until 1500 Doses.
- Develop for 5 minutes.

(2) Fabrication step of 1 mm wide Y branched channel

- After HMDS coating, coating 20-μm-thick PMER on silicon substrate.
- Expose at hard-contact using both a mask and a resist sample until 1000 Doses.
- Develop for 6 minutes.
- Transcribe silicon pattern on PDMS.

Fabricated model patterns were made by same process in capillary vessel models. Model patterns were transcribed onto PDMS substrate, and plasma bonded. And later, we coated PDMS on edge of model and completed microchannels for cell experiment. This model had no leakage and circular cross-sections (Fig. 4.7). We used it for cell incubation experiment. HUVECs were seeded onto 10 μm microchannels and maintained with the same media. Fibronectin made from bovine serum (FN, SIGMA Inc.) is used as an adhesion molecule. The FN was mixed with Dulbecco's phosphate-buffered saline, PBS (-) (final FN conc. 100 μg/ml). Microchannels were prepared before seeding as follows:

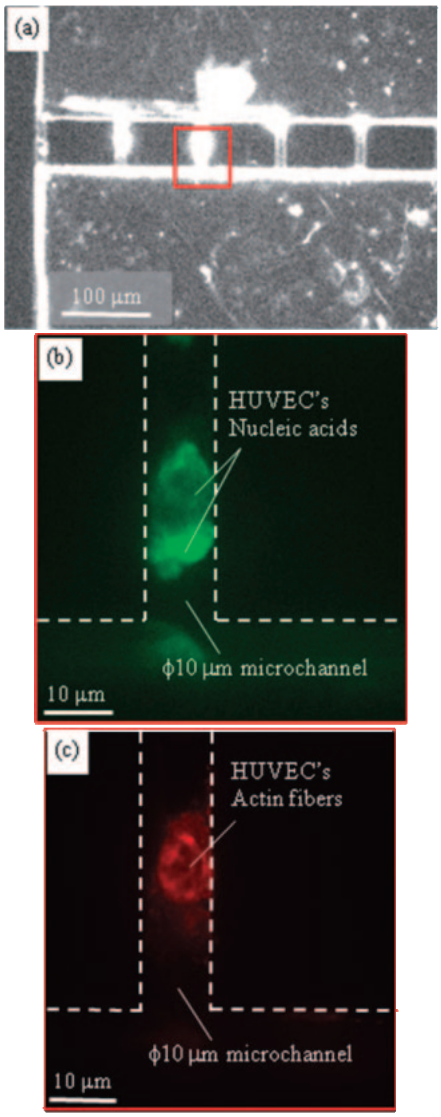

Fig. 4.8. Cell seeding and culture on microchannel. (a) Photograph of the fabricated microchannel three day after HUVECs seeding. (b) Nucleic acid of HUVECs. (c) F-actin of HUVECs. Objective lens: (a) is 10x. (b) and (c) are 60x.

- Wash once in a 100% ethanol.
- Soak in 70% ethanol for 30 min at room temperature.
- Wash in PBS (-) and soak in PBS (-) on a clean bench.
- Continue soaking in PBS (-) at 37°C for 2 hours 10 min after incubation at 60°C in a water bath.
- Immediately remove PBS (-) using dry paper, coat with of FN solutions (200 μl) on a dish and then keep at room temperature for 5 min.

After FN coating, HUVECs were seeded into microchannels, and cultured in the incubator (cells: 1.0 x 10^5/well, 5% CO_2) for 3 days.

The optical microscope (BX62, Olympus Co. Ltd.) used to observe HUVECs on scaffolds has a fluorescent system included two mirrors (blue and green excitation, Olympus), a conventional broadband illumination source, and an electron multiplying CCD (iXon^{EM}, Andor Technology Plc.). We used SYTO 13 Green- Fluorescent Nucleic Acid Stains (Molecular Probes, Inc.) and Phalloidin-rohdamine X conjugate (Wako pure chemical industries, Ltd.) to observe cells on scaffolds. SYTO dyes generally stain nucleic acids. Phalloidin conjugates are used to indicate F-actin behavior such as actin fibers. Microchannels with seeded HUVECs were stained after 3 days of culture. Fluorescent dye for HUVECs on microchannels was prepared as follows:

- Wash the microchannels with growth media.
- Soak in a mixture of 1 μM SYTO13 and media, and incubate at 37°C for 20 min under shading.
- Wash the scaffold twice with growth media.
- Immobilize HUVECs on the microchannels using 4% paraformaldehyde phosphate buffer solution
- Wash with PBS(-), treated with 0.1% Triton X-100, and rewash with PBS(-).
- Soak in a 0.16 μM Phalloidin PBS solution for 20 min at room temperature under shading.
- Wash the scaffold twice with PBS(-).

After cells were dyed, microchannels were exposed to excitation light under microscopy. The absorption of SYTO 13 dye in the presences of DNA/RNA is 488/491nm and the emission wavelength is 509/514 nm. In the presence of F-actin, absorption is 556 nm and the emission wavelength is 574 nm. Figure 4.8 shows images of the patterned PDMS microchannels before seeding and 3 days after cell cultures. The comparison of Fig. 4.8 (a) is photograph of the fabricated microchannels. In Fig. 4.8 (b) (c), green and red sites indicate nucleic acids and actin fibers of cells adhering to the patterns. Comparing these results, HUVEC adhered on inner of 10 μm microchannels.

D. Results and Discussions

We fabricated a capillary vessel model using photolithography (multi stage exposure). We had the problem as capillary vessel model channel's cross-section was very little out of alignment, but we could improve the shape of model channel's cross-section using the assembly alignment patterns. The assembly alignment patterns are very useful when we make the arteriole and capillary vessel model. Moreover, it was confirmed we can make a new resist pattern on the silicon substrate and the resist pattern selectively, and we made semiround resist pattern on the resist pattern using plasma treatment. We observed this channel has no leakage and circular cross-section by the flow experiment.

And, we seeded and observed HUVECs on 10 μm diameter microchannels made by multi stage exposure photolithography.

4.2. Fabrication of Transparent arteriole membrane models

Because of the brittle nature of wax, the surgical simulator model needs to be greater than 500 μm in diameter. However, to better simulate an actual blood vessel environment, blood vessel models smaller than 500 μm in diameter are required. Furthermore, diseases such as arteria basilaris effect blood vessels under ϕ500 μm. Current surgical simulators, therefore, cannot be used for surgical rehearsal and training treatments of such diseases. Thus, a surgical simulator model with ϕ10–500 μm arterioles and capillaries is needed. To address this issue, we designed arteriole and capillary vessel models, as shown in Fig. 4.9. These models were fabricated by photolithography. Figure 4.10 shows the multiscale fabrication methods used for different blood vessel models. We used an over exposure method, a reflow method, gray-scale lithography, and a layer stack molding machine. Among these, the over exposure method, the reflow method, and gray-scale lithography are used to generate fine structures. Due to limits of the fabrication accuracy, however, it is necessary to select the method appropriate for the fabrication of a model with the desired vessel diameter. After exposure, fabricated photoresist patterns are transcribed onto poly(dimethylsiloxane) (PDMS). Arteriole and capillary vessel block models with circular cross-sections are fabricated by bonding two patterned PDMS substrates using plasma treatment and heating.

Block models, however, cannot recreate the moderate compliance needed to mimic that of real blood vessels.

Thus, we believe that the use of arteriole and capillary vessel membrane models as surgical simulators can resolve this problem, and that sacrificial models are needed to improve membrane reproduction. However, because of the brittleness of wax, we were unable to fabricate sacrificial models by the previous fabrication method using a layer stack-molding machine.

In this paper, we propose a novel method for fabricating transparent arteriole membranous models. We attempted to decrease the brittleness of wax by mixing it with PVA (polyvinyl alcohol). After fabricating sacrificial models using this mixture, arteriole membranous models were fabricated by dip coating. The merits of making membranous models smaller than ϕ500 μm for surgical simulation include the following: (1) enables modeling of blood vessel diseases such as arteria basilaris that effect vessels with a diameter of 100 μm, and (2) allows fabrication of high-precision surgical simulators. In this paper, we also report our fabrication method, fabricated arteriole membranous model, and the evaluation results for the molding material (wax and PVA mixture).

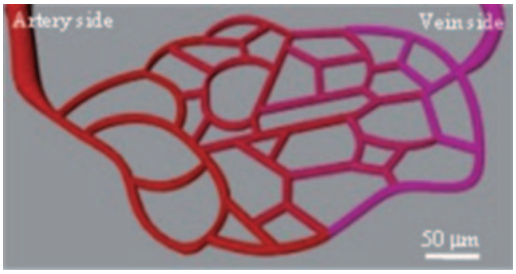

Fig. 4.9. Designed arteriole and capillary vessel model.

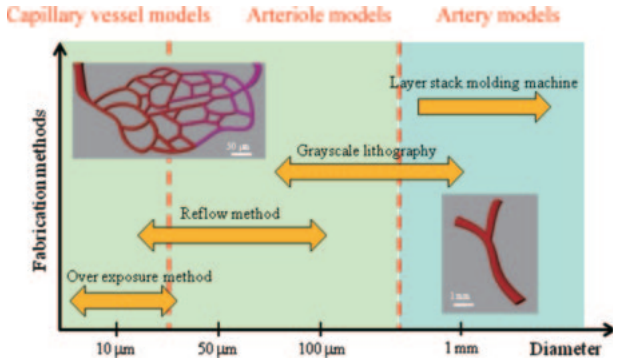

Figure 4.10. Concept of fabrication methods for multi scale blood vessel models.

A. Fabrication of arteriole membrane models

Since wax is fragile, we opted to use a mixture of wax and PVA as a material for our sacrificial model. During the fabrication process of the membrane models, we created model patterns by grayscale lithography and transcribed the resist patterns onto PDMS. We aligned two patterned PDMS substrates filled with the wax and PVA mixture on the patterned side, and dried them at room temperature. We fabricated our sacrificial models, as illustrated in Fig. 4.11. This sacrificial model was coated with PVA to smooth the surface and was later coated with a transparent silicone resin by dip coating to achieve a membranous structure. After dip coating, the sacrificial model and PVA used for smoothing were dissolved by DI water and acetone, leaving a synthetic transparent arteriole membrane, as illustrated in Fig. 4.12. Figure 4.13 shows a ϕ500 μm arteriole membranous model fabricated using this technique. The fabricated model has circular cross-section.

A. Fabrication process of sacrificial models

For fabricating our arteriole membrane models, sacrificial models were needed as molds for dip coating of PVA and silicone resins. We fabricated these sacrificial models with this wax and PVA mixture. Patterned PDMS substrates were fabricated by grayscale lithography with negative photoresist and resist patterns were transcribed onto PDMS for molding the sacrificial models. The fabrication process was as follows:

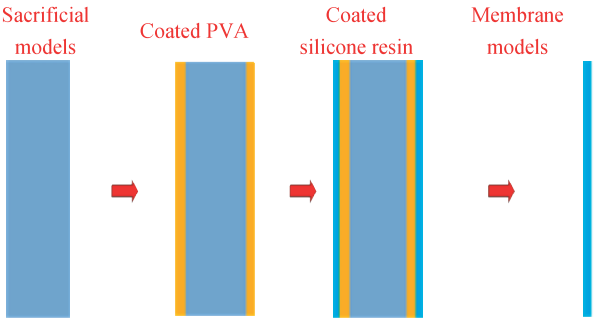

Fig. 4.11. Process chart for sacrificial model.

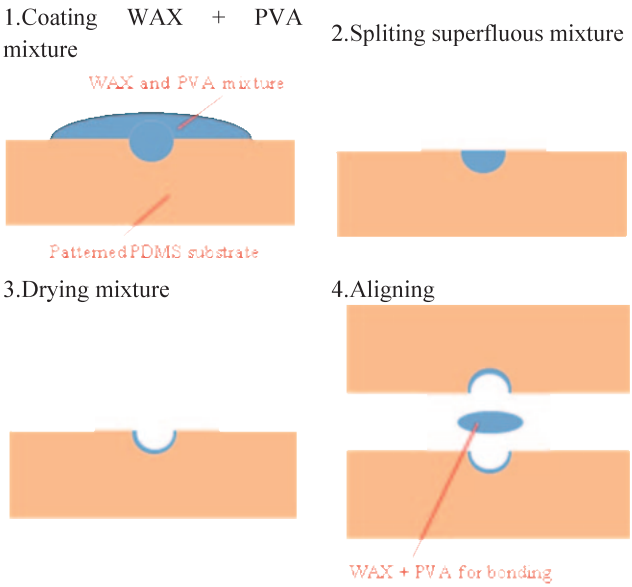

Fig. 4.12. Process chart for membrane model.

A) Grayscale lithography process.

1. Coating photoresist on the glass substrate.
2. Exposure using the best exposure conditions from the backside of the substrate.
3. Development using the best time assessed.
4. Transcribing the resist patterns onto PDMS.

B) Fabrication process used for the sacrificial models (Fig.4.12).

1. Coating the wax and PVA mixture on the patterned side of PDMS substrate.
2. Splitting and removing the superfluous mixture.
3. Aligning and bonding two patterned PDMS substrates filled with the mixture on the patterned side.
4. After drying at room temperature, the PDMS substrates were removed to complete the sacrificial model.

The staking mixture was removed from the sacrificial model.

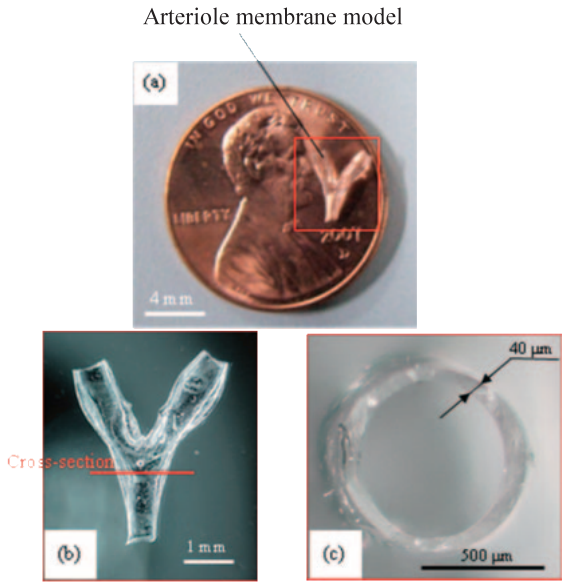

Fig. 4.13. ϕ500 μm arteriole membrane model made by using WAX and PVA mixture material and grayscale lithography. (a)fabricated arteriole membrane model on a cent coin. (b)fabricated arteriole membrane model. (c)cross-section of fabricated arteriole membrane model.

B. Fabrication process of membrane models

We fabricated arteriole membrane models using sacrificial models. The sacrificial model was coated with PVA for smoothing the surface, and was later dip-coated with a transparent silicone resin to achieve a membranous structure. After dip coating, the sacrificial model and PVA for smoothing were dissolved in DI water and acetone resulting in the transparent arteriole membrane model. The fabrication process was as follows.

1. Dip coating of the sacrificial model with a 10wt% PVA solution to smooth the surface.
2. After drying PVA, the sacrificial model was dip-coated with silicone resin.
3. The sacrificial models and PVA used for smoothing were dissolved in a DI water and acetone liquid mixture.
4. The membranous silicone structures were dried to obtain blood vessel membrane models.

Figure 4.13 shows the fabricated arteriole membrane model. We observed that the models had a hollow structure. The arteriole membrane models had circular cross-section (Fig. 4.13 b**)**. The circularity of the inside of the membrane model was calculated by dividing the shortest axis by the longest axis; the calculated circularity of this model was 90%.

B. Evaluation of WAX + PVA mixture materials

For our fabrication process, a wax and PVA mixture was used to build the sacrificial models. These models were useful for fabricating membrane models smaller

Table 1. Experimental rigidity

PVA:WAX ratio [%]	Young's modulus [MPa]
1:0	9.57
4:1	9.69
3:2	8.78
2:3	15.7
1:4	22.8
0:1	20.6

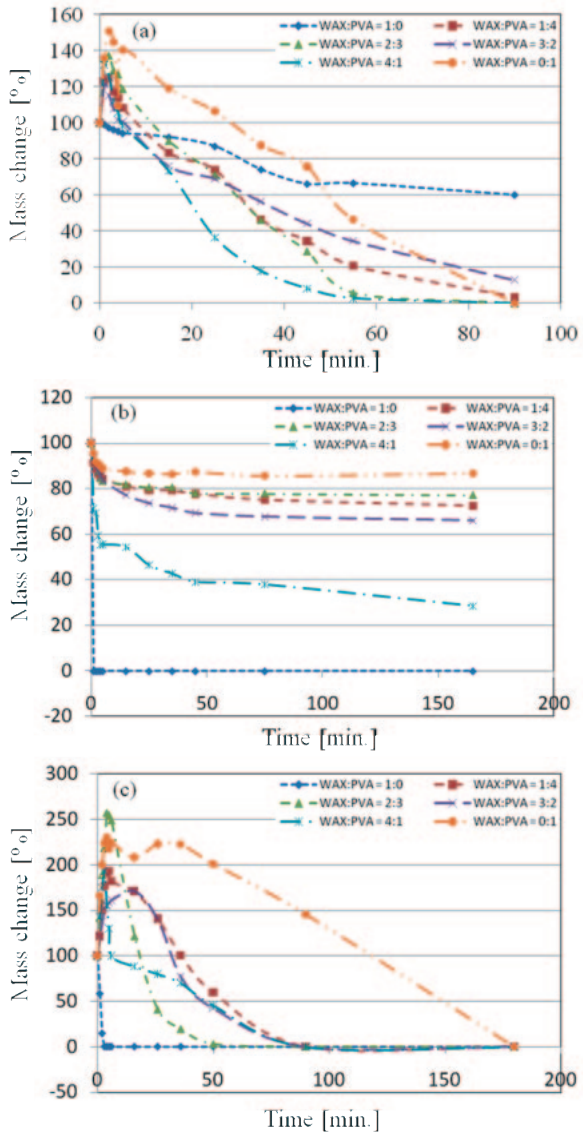

Fig. 4.14. Evaluation of chemical features. (a)DI water (b)acetone (c)acetone + DI water

than 500 μm in diameter. When we used only wax for making the sacrificial models, a certain temperature had to be maintained in order to control the process. Furthermore, the fragility of wax proved unsuitable for our fabrication procedure. On the other hand, when PVA alone was used for making our sacrificial model, the model quickly deformed under its own weight when dip coated because PVA has a low bend strength. Therefore, we propose a mixture of wax and PVA for fabricating sacrificial models. We predict that the mixture has properties of both wax and PVA. We evaluated the properties of the mixture by changing the mix ratio. We evaluated melting time in differentliquids (solubility) and Young's modulus of each mixture made using different mix ratios (wax:PVA = 1:0, 1:4, 2:3, 3:2, 4:1, 0:1).

A. Evaluation of mechanical properties (Young's modulus)

For evaluation experiments, a tensile tester was used to measure Young's modulus. Samples fabricated using our wax and PVA mixture were 50 mm × 10 mm × 2 mm (long × wide × thick) in size. We plotted the measurement results as a load–displacement curve. We conducted the tensile experiment in triplicate for each wax:PVA mix ratio. We calculated Young's modulus using the curve data. Young's modulus for each mix ratio was calculated by averaging the experimental results. Table 1 shows Young's modulus for each mix ratio. Young's modulus using PVA alone was 9.57 MPa, whereas that using only wax was 20.6 MPa. We observed that Young's modulus increased with increasing amount of wax. Extension is an expression of a material's brittleness and ductibility. We observed an increased extension with greater amounts of PVA in the mix. Therefore, we were able to control the mechanical properties of the wax and PVA mixture by changing the mix ratio.

B. Evaluation of chemical properties (solubility)

Melting time of each mix ratio in different liquids was determined by measuring the mass changes. Experiments were conducted to determine the solubility of each mix ratio. We used an ultrasound bath set at 50°C for our solubility experiments. We used DI water, acetone, and a mixture of DI water and acetone as solvents in the experiments. DI water easily melted PVA and acetone easily melted wax. We decided to use a 1:1 acetone to DI water mix to melt the wax and PVA combinations. Figure 4.14 shows the experimental results examining the solubility of each sample in DI water, acetone, and the 1:1 DI water and acetone liquid. Because of the physical characteristics of DI water, the mix samples melted easily. To evaluate our results, we examined the mass changes for wax in the samples. These changes occur due to the heating process and etching effects of the ultrasound bath. Although acetone can melt wax easily, it could only melt a few mixtures in our experiments. This was likely because wax was coated with PVA, so acetone could not reach the wax component of the mixtures. Thus, we assumed that the mixture of wax and PVA would melt easily by the DI water and acetone combination. This was verified by our experiment. Comparing these results, we found that all mixtures of wax and PVA could be melted in the DI water and acetone combination, but the solution rate was not constant. We observed that PVA absorbed DI water

and increased in mass at the beginning of these experiments. Our findings indicate that a 1:1 combination can be used to melt wax and PVA mixed materials.

5. Summary

Mechano-bio systems play an important role to supply advanced devices and equipments for biomedical engineering. For future improvement, it is obvious that micro-nanotechnology plays an important role. Interdisciplinary education as well as research works between engineering, biological and medical fields are promoted.

References

[1] Arai F, et al. High speed random separation of microobject in microchip by laser manipulator and dielectrophoresis. *Proc IEEE Micro Electro Mechanical Systems Conf*, 727-732, 2000.

[2] Arai F, et al. 3D 6DOF Manipulation of Micro-object Using Laser Trapped Microtool. *Proc of 2006 IEEE Int'l Conf on Robotics and Automation*, 1390-1395, 2006.

[3] Arai F, Onda K, et al. Micromanipulation of Microtools Made of SU-8 by Integrated Optical Tweezers. *μ-TAS*, 396-398, 2008.

[4] Yamanishi Y, Lin YC, and Arai F. Magnetically Modified PDMS Devices for Active Microfluidic Control. *μ-TAS*, 883-885, 2007.

[5] Yamanishi Y, Sakuma S, Kihara Y, and Arai F. On-chip Magnetic 3D Soft Microactuators Made by Gray-scale Lithography. *2008 IEEE/RSJ Int Conf on Intelligent Robots and Systems (IROS2008)*, 4054-4059, 2008.

[6] Yamanishi Y, Sakuma S, Onda K, and Arai F. Magnetically Modified Polymeric Microsorter for On-chip Particle Manipulations. *2008 IEEE/RSJ Int Conf on Intelligent Robots and Systems (IROS2008)*, 570-575, 2008.

[7] Azuma D, Narumi K, and Arai F. Fabrication of Articulated Microarm for Endoscsopy by Stacked Microassembly Process (STAMP). In *IEEE MHS '08*, Nagoya, Japan, 396-401, 2008.

[8] Uchida T, et al. Development of biodegradable scaffolds based on patient-specific arterial configuration. *J Biotech* **133**, 213-218, 2008.

[9] Nakano T, Yoshida K, et al. Fabrication of Capillary Vessel Model with Circular Cross-Section and Applications. In *Proc 2008 JSME Conf on Robotics and Mechatronics (ROBOMECH2008)*, Nagano, 2P2-J17, 2008.

[10] Nakano T, Yoshida K, et al. Fabrication of Transparent Arteriole Membrane Models. In *Proc of IEEE MHS '08*, Nagoya, Japan, 457-462, 2008.